JACS
JOURNAL OF THE AMERICAN CHEMICAL SOCIETY
Article
pubs.acs.org/JACS

Modeling Detergent Organization around Aquaporin-0 Using Small-Angle X-ray Scattering

Alice Berthaud,[†,§] John Manzi,[†] Javier Pérez,*[,§,‡] and Stéphanie Mangenot[†,‡]

[†]Institut Curie, Centre de Recherche, CNRS UMR168, Université Pierre et Marie Curie, F-75248 Paris Cedex, France
[§]Synchrotron Soleil, Beamline SWING, Saint Aubin BP48, F-91192 Gif Sur Yvette Cedex, France

Supporting Information

ABSTRACT: Solubilization of integral membrane proteins in aqueous solutions requires the presence of amphiphilic molecules like detergents. The transmembrane region of the proteins is then surrounded by a corona formed by these molecules, ensuring a hydrophilic outer surface. The presence of this corona has strongly hampered structural studies of solubilized membrane proteins by small-angle X-ray scattering (SAXS), a technique frequently used to monitor conformational changes of soluble proteins. Through the online combination of size exclusion chromatography, SAXS, and refractometry, we have determined a precise geometrical model of the *n*-dodecyl *β*-D-maltopyranoside corona surrounding aquaporin-0, the most abundant membrane protein of the eye lens. The SAXS data were well-fitted by a detergent corona shaped in an elliptical toroid around the crystal structure of the protein, similar to the elliptical shape recently reported for nanodiscs (Skar-Gislinge et al. *J. Am. Chem. Soc.***2010**, *132*, 13713−13722). The torus thickness determined from the curve-fitting protocol is in excellent agreement with the thickness of a lipid bilayer, while the number of detergent molecules deduced from the volume of the torus compares well with those obtained on the same sample from refractometry and mass analysis based on SAXS forward scattering. For the first time, the partial specific volume of the detergent surrounding a protein was measured. The present protocol is a crucial step toward future conformational studies of membrane proteins in solution.

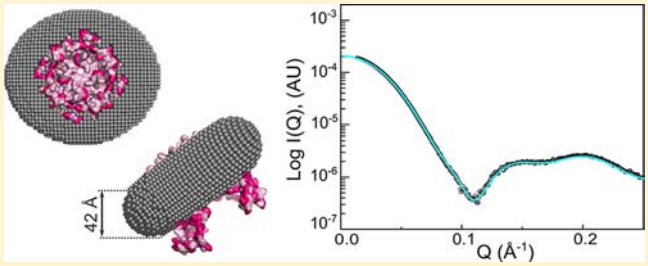

INTRODUCTION

Membrane proteins are involved in many vital processes, including cellular adhesion, bioenergetics, and intracellular communications. Nearly 25% of the genome codes for membrane proteins,[1] and over 50% of these proteins are the target of therapeutic agents,[2,3] thus highlighting the need for a better understanding of their functions and roles in biological processes. Unlike soluble proteins, the surface of an integral membrane protein consists of both hydrophobic and hydrophilic regions. The hydrophobic regions are needed to interact with the lipid alkyl chains in the membrane interior, while the membrane protein surface at the membrane interface and in solution is hydrophilic. This polyphilic character greatly complicates their handling and study. Currently the number of high-resolution atomic structures of membrane proteins is relatively low compared to soluble proteins.[4] However, ongoing efforts to improve crystallization protocols have led to an increasing number of available membrane protein structures. As for soluble proteins, a membrane protein may undergo conformational changes from its crystal structure when performing its function. Additionally, conformational changes or oligomerization of a membrane protein due to changes in the external conditions, such as the presence of ATP or a ligand or change in pH, may also lead to a functional modification.[5−7] Thus, while the static crystallographic structures provide a crucial template, techniques to track conformational changes in membrane proteins will be crucial for understanding their function.

Small-angle X-ray scattering (SAXS) is well suited to monitor ternary or quaternary conformational changes of soluble proteins and has no significant limitation on protein size or molecular weight.[8,9] Although SAXS does not provide molecular-level resolution, it has proven to be particularly useful for distinguishing between different structural models obtained (or proposed) from higher resolution techniques and has become a popular technique among protein crystallographers.[10] SAXS can also be used as an *ab initio* technique to propose possible molecular envelopes for proteins of completely unknown structure. In this case, the algorithms are based on the assumption that a protein possesses a homogeneous electronic density with respect to water, which is effectively true for soluble proteins. In contrast, SAXS has rarely been used for the study of solubilized membrane proteins,[11−13] mainly for the following reasons:

(i) Because of their hydrophobic regions, membrane proteins are not soluble in typical aqueous buffers and require detergent to maintain protein proper folding and avoid aggregation. The amphiphilic detergent molecules form a corona around the transmembrane region of the protein with their polar heads

Received: February 20, 2012
Published: May 23, 2012

   dx.doi.org/10.1021/ja301667n | J. Am. Chem. Soc. 2012, 134, 10080−10088

facing the aqueous medium. In the resulting protein−detergent complex, the protein and detergent corona have very different electron densities. *Ab initio* methods applied to SAXS curves assume a uniform electron density and therefore cannot be applied to SAXS data from membrane protein−detergent complexes.[11]

(ii) For proper solubilization of a membrane protein, the detergent concentration has to be above the detergent critical micellar concentration (cmc),[14] implying that free micelles of detergent coexist in the solution with the protein−detergent complexes. Both the protein−detergent complexes and pure detergent micelles contribute to the measured SAXS data, and the two components have comparable size and scattering power. The precise concentration of the pure detergent micelles is difficult to determine from the total detergent and protein concentrations, as it depends on a complex equilibrium between free detergent molecules, pure detergent micelles, and detergent corona around the protein molecules. It is therefore difficult to isolate the scattering curve arising solely from the protein−detergent complexes, which should be the first step of analysis.

The goal of the present work is to tackle the difficulties caused by the presence of detergent and propose a new method to obtain a complete structural model of the protein−detergent complex consistent with the SAXS data. Unlike in previous studies,[12,13] the combination of SEC−HPLC with SAXS data collection available at the SWING beamline at SOLEIL was used to unambiguously subtract the contribution of the free detergent micelles in solution. The resulting SAXS data were then fitted to a model of the protein−detergent complex using the atomic structure of the membrane protein and a detergent corona modeled as a torus with two predefined electronic densities.

To illustrate our approach, we performed SAXS on aquaporin-0 (AQP0) solubilized in *n*-dodecyl β-D-maltopyranoside (DDM) detergent. The choice of the detergent was crucial and will be discussed later in the paper. AQP0 has a molecular weight of 28 kDa per monomer and is a member of the aquaporin protein family, whose main function is to carry water and small solutes across the membranes. Unlike other aquaporins that are expressed in several tissues, AQP0 is specific to the eye lens, where it represents 60% of all membrane proteins. SAXS was performed on solution of full-length AQP0, which assembles into a tetramer in the membrane. We built a model of the detergent organization around the AQP0. The resulting excellent agreement with the SAXS data clearly surpasses those proposed in similar attempts,[12,13] demonstrating that a major step forward in our ability to analyze SAXS data was overcome. Additionally, our model was combined with refractometry measurements to determine that the AQP0 tetramer is surrounded by around 250 ± 20 molecules of DDM.

The present work shows that it is possible to model the contribution of the detergent corona around the membrane proteins to SAXS data, introducing a new possible way of analyzing conformational changes of membrane proteins by SAXS.

MATERIALS AND METHODS

Sample Preparation. Native Aquaporin-0 (AQP0) was purified from the cortex of sheep lens (INRA, Jouy en Josas, France) as previously described.[15] Briefly, membranes were isolated by several stages of homogenization and centrifugation. Membranes were then solubilized with 4% (w/w) *n*-octyl β-D-glucopyranoside (OG, Anagrade), and the sample was loaded onto a Mono-S 5/50 GL ion-exchange column (GE Healthcare) equilibrated in buffer A: 10 mMTris-HCl pH 8, 0.2% (w/w) DDM (Anagrade, see Figure SI1). AQP0 was then eluted using a gradient from 0% to 100% of buffer B: 10 mMTris-HCl pH 8, 1 M NaCl, 0.2% DDM (w/w). AQP0 eluted at approximately 350 mM NaCl, 10 mM Tris-HCl (pH 8), 0.2% DDM

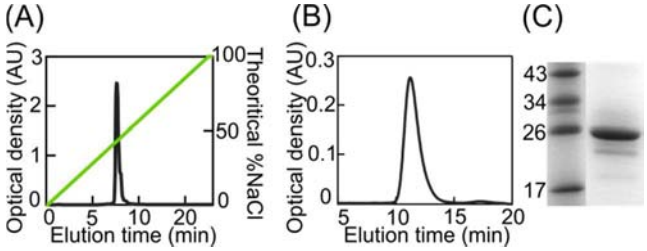

Figure 1. (A) Elution profile of the ion-exchange Mono-S column equilibrated in buffer A (10 mM Tris-HCl pH 8, 0.2% (w/w) DDM) as a gradient from 0% to 100% of buffer B (10 mM Tris-HCl pH 8, 1 M NaCl, 0.2% (w/w) DDM (green line)) was applied to the column. The AQP0 eluted at approximately 350 mM NaCl, 10 mM Tris-HCl pH 8, 0.2% (w/w) DDM. (B) Elution profile of the AQP0 on a gel filtration Superose 12 column equilibrated with 10 mM Tris pH 8, 150 mM NaCl, 0.2% (w/w) DDM. (C) The eluted protein runs as a single band on a SDS−PAGE gel.

(w/w). The elution profile is presented in Figure 1A. The fractions containing the AQP0 were pooled and loaded onto a Superose12 10/300 GL column (GE Healthcare) pre-equilibrated with 10 mM Tris-HCl pH 8, 150 mM NaCl, 0.2% DDM (w/w) (elution profile presented in Figure1B). To ensure that all the OG was exchanged, the AQP0 fractions were pooled and dialyzed against 10 mM Tris-HCl (pH 8), 150 mM NaCl, 0.2% DDM (w/w) for 1 week at 4 °C. The sample was then concentrated using an Amicon Ultra centrifugal filter concentrator with a 10 kDa molecular weight cutoff (Millipore). This operation concentrated both the AQP0 solution and the free micelles of detergent whose size is reported to be around 70 kDa.[16] The DDM concentration in the final solution was estimated to be around 0.6% (w/w), while the AQP0 concentration was 6 g·L^{-1} as measured by ultraviolet (UV) absorbance at 280 nm using $A_{280} = \varepsilon_{AQP0} = 1.40$ cm^2·mg^{-1} (DDM has negligible absorbance at this wavelength). The integrity of the AQP0 was checked on a SDS−PAGE gel (Figure1C), and the apparent mass was approximately equal to the theoretical mass of an AQP0 monomer (28 kDa).[17]

Small-Angle X-ray Scattering Experiments. SAXS experiments were performed on the SWING beamline at SOLEIL, the French synchrotron facility. The X-ray wavelength (λ = 1.03 Å) and sample-to-detector distance (D = 1845 mm) corresponded to a scattering wave-vector range of 0.013 Å^{-1} < Q < 0.5 Å^{-1}, where $Q = 4\pi \sin\theta/\lambda$ and 2θ is the scattering angle. The solution samples were flowed through a thin-walled 1.5 mm diameter quartz capillary inserted in a vacuum chamber, and scattering data were collected using a 17 × 17 cm^2 low-noise AVIEX CCD detector.

The solution temperature was held constant at 10 °C, and solution flow was controlled by an Agilent high-performance liquid chromatography (HPLC) system configured so that samples passed sequentially through the size exclusion chromatography (SEC) column, a UV−vis cell to measure protein concentration (via UV absorbance at 280 nm), the SAXS flow cell,[18] and a refractometer (Optilab T-rEX, Wyatt Technology). Data were collected using two different SEC columns. For the first one, a SHODEX KW403-07, the column and refractometer blank cell were pre-equilibrated for 3 h with 0.2% DDM (w/w), 10 mM Tris-HCl (pH 7.5), 150 mM NaCl solution at a flow rate of 250 μL·min^{-1}. The flow rate was then set to 150 μL·min^{-1}, and 20 μL of the AQP0 solution was injected onto the column. A total of 256 SAXS images were collected during the elution,

dx.doi.org/10.1021/ja301667n | J. Am. Chem. Soc. 2012, 134, 10080−10088

with a frame duration of 2 s and dead time of 1 s between frames. Using the Foxtrot program, images were radially averaged, divided by the transmitted intensity, and normalized to absolute units with water scattering as a reference. The first 49 frames, corresponding to the DDM elution buffer, were averaged to provide a low noise buffer signal. A total of 35 frames were recorded during the elution peak of the protein−detergent complex, and the signal from the protein−detergent complex was obtained by subtracting the DDM elution buffer signal. No variation of the radius of gyration, R_g, was observed throughout the elution of the protein−detergent complex, and the resulting curves were identical within statistical noise (see Figure SI3). The 12 curves with higher statistics were averaged to improve the signal-to-noise ratio for the final protein−detergent complex scattering curve (see Figure SI3a). Scattering from the detergent in excess in the loading buffer was also recorded and resembled the published scattering profile of DDM micelles[19] (data not shown).

To reduce the peak widening between the optical density (OD) measurement (UV absorbance at 280 nm) and SAXS cell, we performed a second run at higher flow rate using a larger Superose 12 10/300 SEC column (GE Healthcare), but without the refractometer. The column was pre-equilibrated for 40 min with a 0.2% DDM, 10 mM Tris-HCl (pH 7.5), and 150 mM NaCl solution at a flow rate of 500 μL·min^{-1}. The flow rate was then set to 350 μL·min^{-1} for the elution experiment, and 400 μL of the AQP0 solution was loaded onto the column. A total of 256 SAXS images were collected during the elution, with a frame duration of 2.5 s and a dead time of 1 s between frames. The same data analysis procedure was used to obtain the SAXS signal of the protein−detergent complex. The curves obtained with the two columns were found to be identical (data not shown).

Guinier Analysis. For an ideal solution, the radius of gyration of the complex, R_g, and the extrapolated intensity, $I(0)$, at zero scattering angle can be estimated using the Guinier approximation valid at very small angles ($QR_g < 1.2$).[20,21]

$$I(Q) = I(0)\exp\left(-\frac{Q^2 R_g^{\,2}}{3}\right) \tag{1}$$

In this expression $I(0)$, given in absolute units, is related to the complex mass and density by the relation

$$I(0) = \frac{CM}{N_A} f^2 \left(\frac{nN_A}{M} - \rho_0 \bar{v}\right)^2 \tag{2}$$

where C is the complex mass concentration, M is the molar weight of the complex, N_A is Avogadro's number, $f = 2.818 \times 10^{-15}$ m is the classical scattering length of the electron, n is the number of electrons in the dry complex, ρ_0 is the electronic density of the buffer, and $\bar{v}$ is the partial specific volume of the complex. In the case of a complex formed by a membrane protein surrounded by a corona of detergent, $I(0)$ can be directly related to the number, N_{det}, of detergent molecules in the corona. Denoting M_{prot}, n_{prot}, $\bar{v}_{prot}$, M_{det}, n_{det}, and $\bar{v}_{det}$ as the molar mass, molecular number of electrons, and specific volume of the protein and of one molecule of detergent respectively, eq 2 can be reformulated replacing M by $M_{prot} + N_{det}M_{det}$, C by $C_{prot}(1 + N_{det}M_{det}/M_{prot})$, $\bar{v}$ by $(\bar{v}_{prot}M_{prot} + \bar{v}_{det}N_{det}M_{det})/(M_{prot} + N_{det}M_{det})$, and n by $n_{prot} + N_{det}n_{det}$. N_{det} can then be expressed as a function of the ratio between $I(0)$ and the protein mass concentration, C_{prot}:

$$N_{det} = \frac{\sqrt{\frac{I(0)M_{prot}N_A}{C_{prot}f^2}} - (n_{prot}N_A - \rho_s\bar{v}_{prot}M_{prot})}{(n_{det}N_A - \rho_s\bar{v}_{det}M_{det})} \tag{3}$$

Model of Detergent Corona. Models of the AQP0−detergent complex were developed to fit the experimental SAXS curve. The protein tetramer was represented by its all-atom structure, taken without further modification from the PDB entry 2b6p. In contrast, the detergent corona was modeled using a coarse-grained approach illustrated in Figure 3. The different electronic densities of the hydrophobic and hydrophilic regions of the corona were described by placing two types of pseudo-atom (see below) onto the nodes of two densely packed cubic lattices. The hydrophobic region of the detergent corona, corresponding to the hydrocarbon tails of the detergent, was modeled as an elliptical hollow torus, $T(a,b,e)$, of height a and cross-sectional minor and major axes, b/e and be, where e is the ellipticity of the torus in the plane of the membrane (xy plane). The torus was centered on the symmetry axis (z-axis) of the protein and positioned at the transmembrane region of the protein (see Figure 3). The torus exterior had a radius of curvature, R_T, that was half the torus height ($R_T = a/2$), while the interior surface of the corona was made to precisely follow the surface of the protein by eliminating all pseudo-atoms that overlapped with the protein. The hydrophilic shell of the corona, corresponding to the polar headgroups of the detergent, was modeled as an additional layer of thickness t around the inner torus.

The program Crysol[22] was then used to calculate the SAXS profile for the model. The two types of pseudo-atom, which represented the headgroup and tail regions of the detergent corona, were selected from the Crysol internal database, composed of 20 possible pseudo-atoms. In Crysol, each pseudo-atom is characterized by its number of electrons, n_{e^-}, and its tabulated atomic excluded volume V_{vdW}. The average electronic density of a cubic lattice occupied by a pseudo-atom is then calculated as

$$\rho = \frac{n_{e^-} - V_{vdW}\rho_0}{V_{unit\ cell}} + \rho_0 \tag{4}$$

where ρ_0 is the buffer electronic density, and $V_{uniy\ cell}$ is the volume of the lattice unit cell.

The hydrophobic core of the detergent corona, shown in light gray in Figure 3, was modeled by a network of CH_3 pseudo-atoms ($ne^- = 9$, $V_{vdW} = 31.89$ Å) on a lattice with a unit cell size of 3.17 Å. The corresponding electron density, $\rho = 0.282$ e/Å^3, was close to the previously published electron density for the tail region of the DDM molecule, $\rho = 0.277$ e/Å^3.[19] The hydrophilic shell of the detergent corona, shown in dark gray in Figure 4, was modeled by a network of NH_3 pseudo-atoms ($ne^- = 10$, $V_{vdW} = 17.94$ Å). With the default unit cell size of 2.62 Å, the electron density, $\rho = 0.557$ e/Å^3, was close to the published value for the headgroup region of the DDM of $\rho = 0.522$ e/Å^3.[19] However, the density was matched exactly by adjusting the value of the unit cell size to 2.78 Å. Both CH_3 and NH_3 were chosen within the Crysol table on the basis of their respective intrinsic electron densities (ne^-/V_{vdW}) being the closest to the desired densities. It is thus ensured that the parameters of the grids used to generate the corona model are close to the actual volumes of the chosen groups. In this way, we avoid using a grid either too thin or too loose. To validate this choice, we verified that the theoretical curve from a core−shell ellipsoid model could be perfectly reproduced using a coarse-grained model based on the same grids (see SI2).

In Crysol, the scattering intensity of an assembly of atoms at $Q = Q_i$ is calculated using the expression

$$I_{calc}(Q_i) = \langle |A_{at}(Q_i) - \rho_0 A_{excl}(Q_i) + \delta\rho A_{border}(Q_i)|^2 \rangle_\Omega \tag{5}$$

where $A_{at}(Q_i)$ is the scattering amplitude of the atomic assembly *in vacuo*, ρ_0 is the buffer electron density, $A_{excl}(Q_i)$ is the scattering amplitude of the excluded volume, $A_{border}(Q_i)$ is the scattering amplitude of a hydration layer with a fitted electron density contrast $\delta\rho$, and $\langle\ \rangle_\Omega$ represents an orientational average. While these functions can be directly computed from the model, Crysol also includes two parameters, V_{excl}^{fit} and R_A^{fit}, to fit the experimental data (in addition to $\delta\rho$). These two parameters are linked to the total excluded volume V_{excl}^{calc} and the average atomic radius R_A^{calc}, directly computed from the list of the atoms in the models, with

$$\alpha(V_{excl}^{fit}) = \frac{V_{excl}^{fit}}{V_{excl}^{calc}} \quad \text{and}$$
$$\beta(R_A^{fit}) = \exp(-(4\pi/3)^2 \pi Q_i^{\,2}(R_A^{fit^2} - R_A^{calc^2})) \tag{6}$$

Including these parameters, the calculated intensity is then given by

$$I_{calc}(Q_i) = \langle |A_{at}(Q_i) - \alpha(V_{excl}^{fit})\beta(R_A^{fit})\rho_0 A_{excl}(Q_i) + \delta\rho A_{border}(Q_i)|^2 \rangle_\Omega \quad (7)$$

Note if the models were exact then $V_{excl}^{fit} = V_{excl}^{calc}$ and $R_A^{fit} = R_A^{calc}$, and $\alpha(V_{excl}^{fit})$ and $\beta(R_A^{fit})$, would both be equal to 1. In practice, these two extra fitting parameters compensate for errors in the tabulated atomic radii. In the present work, β was systematically fixed at 1 (by forcing $R_A^{fit} = R_A^{calc}$), and $\alpha(V_{excl}^{fit})$ was restricted between 0.97 and 1.03. The fitting procedure then consisted in minimizing the functional

$$\chi^2(c, V_{excl}^{fit}, \delta\rho) = \frac{1}{N}\sum_{i=1}^{n} \frac{(I_{exp}(Q_i) - cI_{calc}(Q_i))^2}{(\sigma_i)^2} \quad (8)$$

where N is the number of experimental values, $I_{exp}(Q_i)$ is the experimental intensity at $Q = Q_i$, $I_{calc}(Q_i)$ is given by eq 7 and $\beta = 1$, c is a scaling constant, and σ_i is the experimental uncertainty at $Q = Q_i$.

After the fitting procedure, the electron density of a corona pseudo-atom is given by

$$\rho_{fit} = \frac{n_{e^-} - \alpha V_{ndW}\rho_0}{V_{unit\ cell}} + \rho_0 \quad (9)$$

where α is the fitting parameter described in eq 6.

Refractometry Experiments. The refractive index (RI) signal of the protein−detergent complex is given by

$$RI = Cc[\varphi(dn/dc)_{AQP0} + (1 - \varphi)(dn/dc)_{det}] \quad (10)$$

where Cc is the weight concentration of the AQP0−detergent complex, φ is the mass fraction of protein within the complex, and $(dn/dc)_{AQP0}$ and $(dn/dc)_{det}$ correspond respectively to the RI increments of the protein and detergent. The latter values are equal to 0.187 mL·g^{-1} for a protein[23] and 0.143 mL·g^{-1} for the DDM.[23,24]

In the experimental setup, the solution $OD_{280\ nm}$ was measured before the solution entered the SAXS flow cell while the RI was measured after the solution left the flow cell. To calculate the protein concentration in the refractometer, the raw OD profile was convoluted by a specific delay function using the ASTRA 5.3.4 software (Wyatt Technologies). After this correction, the OD and weight concentration, Cc, are related by

$$Cc = \frac{OD}{\varphi\varepsilon_{AQP0}} \quad (11)$$

Combining eqs 10 and 11, the protein mass fraction of the complex is then

$$\varphi = \frac{OD(dn/dc)_{det}}{\varepsilon_{AQP0}}\left[RI - \frac{OD[(dn/dc)_{prot} - (dn/dc)_{det}]}{\varepsilon_{AQP0}}\right]^{-1} \quad (12)$$

Finally, the number of detergent molecules in the complex, N_{det}, is given by

$$N_{det} = \frac{(1 - \varphi)}{\varphi}\frac{M_{prot}}{M_{det}} \quad (13)$$

where M_{prot} is the molar protein mass and M_{det} is the detergent molar mass.

RESULTS

Figure 2A shows the UV absorption at 280 nm (black) and RI variation (yellow) signals for a 6 mg·mL^{-1} solution of AQP0 (in approximately 0.6% DDM) eluted through a SHODEX SEC-HPLC column using a 0.2% DDM buffer. Both profiles display three different zones corresponding respectively to the pure elution buffer (zone 1), a small fraction of aggregated proteins (zone 2) and the isolated AQP0−detergent complex (zone 3). Most of the protein (approximately 95%) eluted as a

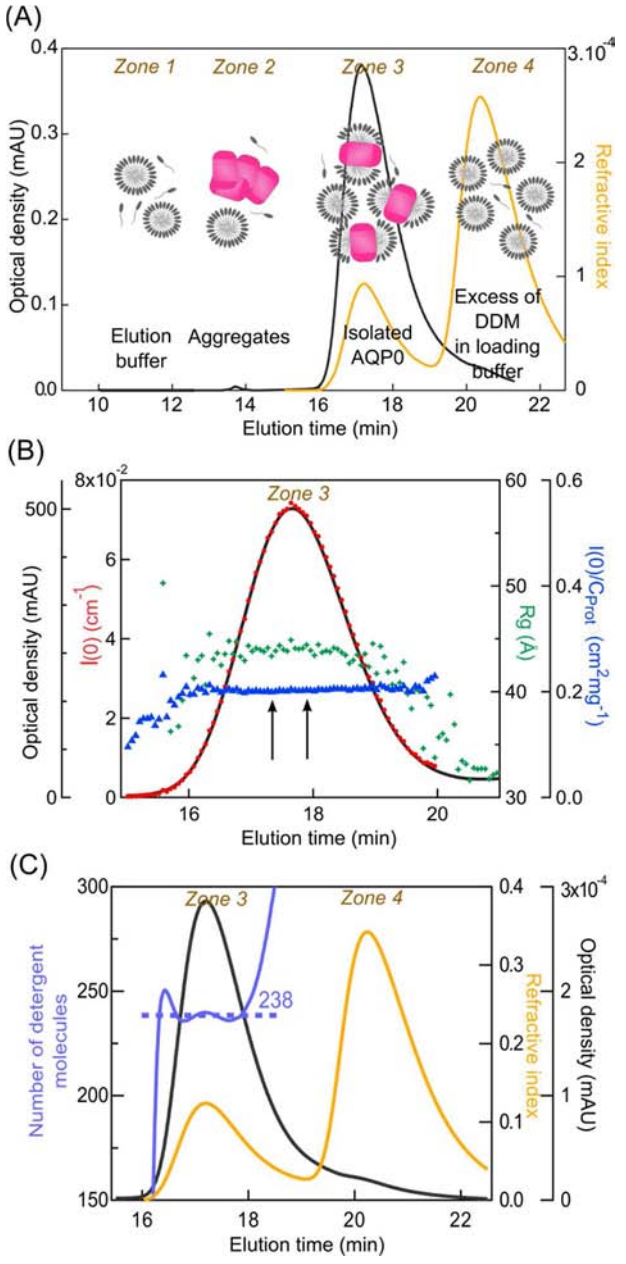

Figure 2. (A) Elution profile of the protein detergent complex measured by OD at 280 nm (black line) and refractometry (yellow line) using the SHODEX column with a flow rate of 150 μL·min^{-1}. The refractometer reference cell was previously equilibrated with the elution buffer (10 mM Tris-HCL pH 8, 150 mM NaCl, 0.2% (w/w) DDM). The OD signal was convoluted by the delay function from the software ASTRA (Wyatt Technology) to account for the peak widening effect. The four zones respectively correspond to the elution buffer (1), protein aggregates (2), AQP0 (3), and excess detergent in the loading buffer (4). (B) Elution profile of the protein detergent complex using the Superose 12 column with a flow rate of 350 μL·min^{-1}. Black line: OD at 280 nm. Red dots: $I(0)$, SAXS intensity extrapolated at $Q = 0$. Green dots: radius of gyration, R_g. Blue dots: ratio between $I(0)$ and C_{prot} (deduced from OD). The OD signal was not convolved with a delay function. (C) Zoom on zones 3 and 4: Number of detergent molecules in the AQP0−detergent complex calculated from eq 13 (blue line). In the protein elution peak the number of detergent molecules is constant and equal to 238 ± 15 DDM molecules (blue dotted line).

dx.doi.org/10.1021/ja301667n | J. Am. Chem. Soc. 2012, 134, 10080−10088

well-defined peak (zone 3) suggesting that a single protein species was present in the injected solution. The refractometry profile displays an additional peak (zone 4 in Figure 2A), not detected by UV absorption, which is due to the excess of detergent in the loading buffer ($(dn/dc)_{det}$ = 0.143 mL·g^{-1}). The excess DDM peak is clearly separated from the peak of the protein−detergent complex, meaning that SAXS signal from the complex can be effectively isolated from SAXS from additional DDM micelles.

Buffer subtraction is a crucial step when measuring SAXS from a protein solution. Correct subtraction is especially challenging for solubilized membrane proteins because the elution buffer contains detergent above its cmc, unlike a soluble protein buffer which contains only salts. In the present work, AQP0 was solubilized in 4% (w/w) OG buffer as OG is known to be very efficient for membrane solubilization.[25] The OG was then replaced by DDM 0.2% (w/w) because DDM has a lower cmc value of 8.5 × 10^{-3} %. However, despite lowering the detergent concentration, the SAXS signal recorded during the elution of the protein (zone 3 in Figure2A) still includes contributions from both the protein−detergent complex and the free micelles in solution. As mentioned in Materials and Methods, one of the advantages of the online HPLC equipment on the SWING beamline is that it separates the protein−detergent complexes (eluting in zone 3) from excess detergent in the loading buffer (zone 4). The free detergent micelle concentration eluting with the protein−detergent complex is then identical to the concentration in the elution buffer (0.2% DDM in 10 mM Tris-HCl pH 7.5, NaCl 150 mM). Thus, the buffer signal can be determined by averaging the 49 frames prior to the elution of the AQP0−DDM complexes (zone 1 in Figure 2A). The SAXS profile from the excess DDM micelles in the loading buffer was calculated by subtracting the signal recorded in zone 4 from the buffer signal and the result (data not shown) was similar to previously published SAXS measurements of pure DDM micelles.[19]

To evaluate the AQP0−detergent complex mass, $I(0)$ was calculated by extrapolation of eq 1, and the result compared to the AQP0 concentration, C_{prot}, measured by UV absorption at 280 nm. However, when the flow rate was low the measured value of $I(0)/C$ was not constant because of peak widening between the OD and SAXS cells. To avoid this effect and only to record the $I(0)/C$ value, the experiment was repeated using a higher flow rate and larger Superose12 10/300 column (GE Healthcare). As shown in Figure 2B, at the higher flow rate $I(0)$ and C_{prot} are proportional with a constant value of $I(0)/C_{prot}$.

Equation 2 therefore implies that the protein−detergent complex mass is constant throughout the elution and that there is no significant depletion of detergent. The radius of gyration, R_g (green, Figure 2B), also remains constant throughout the elution of the protein−detergent complex (R_g = 43.8 ± 0.5 Å), meaning that the overall size of the complex remains constant and thus confirming that the protein detergent complex eluted as a single monodisperse species.[18] The frames recorded during the protein elution (delimited by arrows in zone 3 in Figure 2B) were then averaged (see Figure 4, dark gray dotted line), and the resulting scattering curve (Figure 4, black dotted line) was used for further analysis. Before averaging, the individual frames were checked to be identical in the whole Q-range within statistical noise (see Figure SI3).

The AQP0−detergent complex curve displays a linear Guinier plot confirming the absence of aggregates (inset in Figure 4). The whole curve is characterized by a strongly modulated shape with a pronounced minimum at Q = 0.11 Å^{-1} and two secondary maxima at Q = 0.15 and 0.20 Å^{-1}. In the following section, the experimental scattering is compared to a structural model of the protein−detergent complex in which the protein is represented by its known crystal structure and the detergent corona modeled using a coarse-grained approach.

Coarse-Grained Model Simulation of the Detergent Corona. The detergent was first modeled by a torus of circular section characterized by three geometrical parameters a, b, and t (Figure 3B,C). Pseudo-atoms with electron densities of 0.282 and 0.522 e/Å^3 were used to represent the electron densities of the detergent headgroup and tail[19] and during the fitting procedure these electron densities were refined by changing the value of the parameter α. The three geometric parameters were sequentially varied (a and b varied by steps of 1 Å, and t varied by steps of 0.5 Å). Crysol was used to fit the resulting model of the protein−detergent complex to the experimental data. Agreement between the experimental and the simulated curves was evaluated both by visual inspection and χ values. Examples illustrating the dependence of χ on a, b and t are presented in Table SI4.

The lowest χ-value (χ = 2.29) was achieved for a = 30 Å, b = 36 Å, and t = 5.5 Å. With these parameters, α = 1.02 corresponding to electron densities of 0.275 [3] and 0.506 e/Å^3 for the DDM hydrophobic and hydrophilic regions, respectively. The quality of the fit depends sensitively on the parameters, as a small change of a or b increases χ significantly (see also Supporting Information SI6). Moreover the values obtained for a and t are compatible with the estimated length of a DDM molecule. In particular, the length of the DDM headgroup is known to be around 6−7 Å, which agrees well with the optimized value reported here (t = 5.5 Å).

Concomitantly the electron densities were only slightly adjusted by the fitting procedure and remain within an acceptable range. The resulting SAXS curve is presented in Figure 4 (red line) on top of the experimental curve (dotted curve). The agreement is particularly good at low Q, and the positions of the first minimum and the two experimental secondary maxima are well reproduced by the model. However, the modulations around the secondary maxima and the minimum at 0.11 Å^{-1} are too pronounced, suggesting that the symmetry of the model is too high.

To better fit the data, the model symmetry was slightly decreased by changing the detergent corona torus from a circular section to an ellipsoidal section (Figure 3D). This introduces an additional geometrical parameter, e, independent of a, b, and t, reflecting the ellipticity of the corona. In a first step, a wide sampling of the four geometrical parameters a, b, t, and e was performed. As for the circular model, a, b, t, and e were systematically varied to find the optimal fit. Initially, a was varied from 24 to 32 Å with steps of 1 Å, b from 33 to 39 Å with steps of 1 Å, t from 0 to 7 Å in steps of 0.5 Å, and e from 1 to 1.3 with steps of 0.1. In a second round, the parameters were varied with smaller steps (0.2 Å for a and b and 0.02 for e) around the optimal values. Table SI5 displays the dependence of χ on the geometrical parameters. As four parameters were independently tuned, the table only shows some of the results around the minimum χ value of 1.37, corresponding to a = 30 Å, b = 35 Å, t = 5.5 Å, and e = 1.12. The χ value for the elliptical model is clearly lower than the circular model, and the improvement in the fit (blue curve) is readily visible in Figure 4. The parameter α was 1.03, which corresponds to electron densities of 0.274 e/Å^3 for the hydrophobic part and 0.504 e/

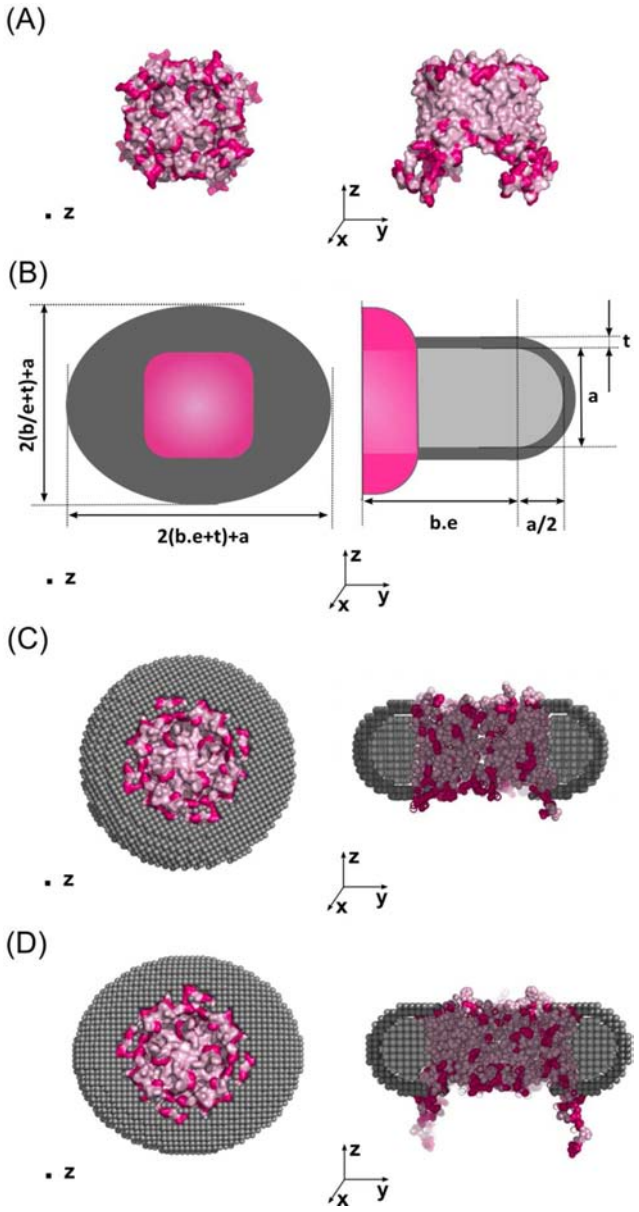

Figure 3. Three-dimensional representations of the AQP0 tetramer and its complex with DDM Left: Top view of the lipid bilayer plane. Right: Side view of the lipid bilayer plane. (A) Atomic structure of the AQP0 tetramer (pdb entry 2b6p) represented in surface mode and colored according to residue hydrophobicity (dark pink, hydrophilic; light pink, hydrophobic). (B) Definition of the torus parameters. The hydrophobic core of the detergent corona is modeled as an elliptical torus of minor and major semi axes b/e and be and height a (light gray), surrounded by a hydrophilic shell of thickness t (dark gray). (C,D) Circular and elliptical coarse-grained models. The detergent lattice around the AQP0 is represented in light gray (hydrophobic) and dark gray (hydrophilic) spheres with different electronic densities. The geometrical parameters of the torus were systematically varied to achieve the best fit between experimental and simulated SAXS data. The resulting best-fitting models are shown. The side view of the cylindrical/elliptical model (D) is represented with a section inside the detergent corona.

Å^3 for the hydrophilic part of the DDM. These values are almost identical to the cylindrical model and only slightly below the literature values for free micelles.[19]

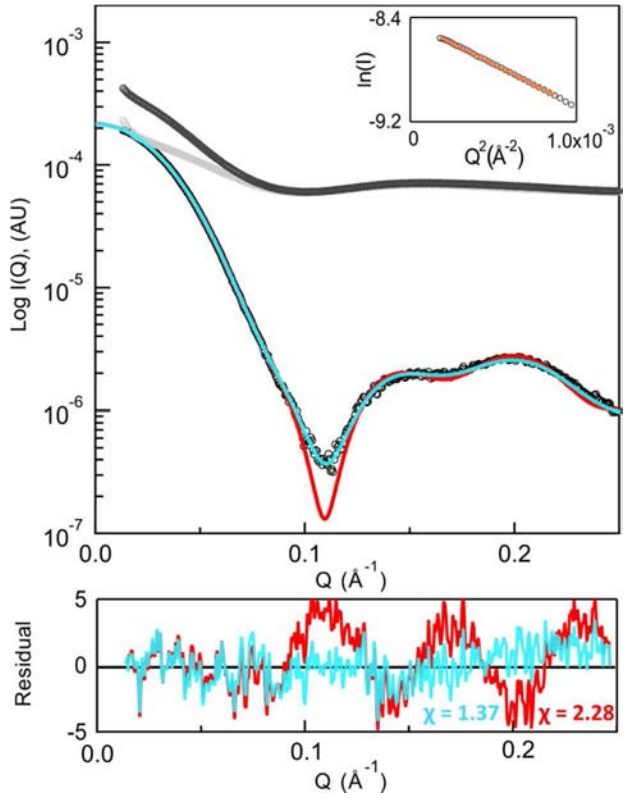

Figure 4. SAXS signal of the AQP0 surrounded by its detergent corona (black dots). The contribution from free detergent micelles (top light gray curve) has been subtracted from the raw data (top dark curve). The red line is the best fitting curve from the complex with a cylindrical detergent torus. The blue line is the best fitting curve from the complex with an elliptical detergent torus. The standard deviation normalized residuals between the experimental and simulated curves are indicated. Inset: Guinier plot of the inner part of the curve. The Guinier fit gave R_g = 44.0 ± 0.2 Å and was performed in the range 0.013 < Q < 0.03 Å^{-1}, corresponding to a reduced range of 0.57 < QR_g < 1.3.

Number of Molecules in the Detergent Corona. The number of detergent molecules represented by the torus model should correspond to number of DDM molecules around AQP0. In the elliptical model, the best fit was obtained with 4335 pseudo-atoms in the head region and 3150 pseudo-atoms in the tail region of the detergent corona. Taking into account the electronic densities and grid unit cell of each region of the torus, these numbers correspond respectively to 47 963 and 27 642 electrons. Since the headgroup of DDM ($C_{12}H_{21}O_{11}$) contains 181 electrons, the number of electrons in the hydrophilic part of the detergent corona corresponds to 265 DDM headgroups. Similarly, the number of the electrons in the hydrophobic part of the detergent corona corresponds to 285 DDM tails ($C_{12}H_{25}$, 97 electrons). Clearly the number of DDM molecules in the core and shell of the corona should be equal, and the discrepancy between the two values is probably due to the abrupt discontinuity in the electronic densities in our model. However, the fact that these two numbers are extremely close strongly supports the validity of the model. Calculating the numbers of detergent molecules from models with χ < 2.3, on average there are 271 ± 30 detergent molecules of DDM around the AQP0.

The number of DDM molecules in the corona can be independently calculated from SAXS data using $I(0)/C$ and eq

dx.doi.org/10.1021/ja301667n | J. Am. Chem. Soc. 2012, 134, 10080−10088

3. Taking the value of $I(0)/C_{prot}$ as 0.203 ± 0.007 (Figure 2B), and literature values for the partial specific volume of AQP0,[23] $\bar{v}_{prot}$ = 0.75 $cm^3 \cdot g^{-1}$, and DDM,[24] $\bar{v}_{det}$ = 0.837 $cm^3 \cdot g^{-1}$, the corona contains 211 ± 10 DDM molecules. The value for the partial specific volume of the DDM was taken from recently published papers. Earlier published values[14] have ranged from 0.800 to 0.837 $cm^3 \cdot g^{-1}$, which would result in a variation of detergent molecules number from 168 ± 10 to 211 ± 10. Interestingly, the partial specific volume of the DDM derived directly from the optimized coarse-grained model is 0.845 ± 0.005 $cm^3 \cdot g^{-1}$, and using this value in eq 3 results in a corona with 224 ± 15 DDM molecules.

Finally, as a third method, the number of DDM molecules in the corona can be independently determined using a combination of UV absorption and RI measurements and eqs 10−13. As shown in Figure 2C, the number of DDM molecules (blue curve) surrounding AQP0 during the elution remains constant and is equal to 238 ± 15.

DISCUSSION

Membrane proteins are not soluble in typical buffers and require the addition of a detergent above its cmc. In the present work, we performed SAXS on a solution of aquaporin-0, the most abundant membrane protein of the eye lens, solubilized in a solution of DDM. Because we were able to isolate the SAXS signal from the protein−detergent complexes, we could accurately fit the SAXS curve to a model of the protein−detergent complex.

Above its cmc, a detergent solution contains micelles whose size is similar to protein−detergent complexes, and these micelles can contribute strongly to the SAXS signal (see Figure 4; both top gray curves). It is therefore crucial to use solubilization conditions that minimize free micelle scattering if one wants to accurately measure the scattering from protein−detergent complexes. The best way to obtain a reproducible low concentration of free micelles is to use a low cmc detergent. A number of different detergents have been used to maintain the proper conformation of membrane proteins including *N*,*N*-dimethyl-dodecylamine *N*-oxide (DDAO or LDAO; cmc = 2 mM), *n*-octyl β-D-glucopyranoside (OG; cmc = 18−20 mM), *n*-decyl β-D-maltopyranoside (DM; cmc = 1.8 mM), and *n*-dodecyl β-D-maltopyranoside (DDM; cmc = 0.17 mM). Since DDM has the lowest cmc, we performed our SAXS data using a 0.2% (w/w) DDM, above its cmc. However, the native eye lens membrane was solubilized with OG, as this detergent is known to be more efficient for solubilizing native membrane proteins. We then took great care to exchange all the OG around aquaporin-0 by performing a series of FPLC experiments and extensive dialysis in DDM buffer. Moreover, it is important to note that the addition of detergent completely removes all the lipids[26] around AQP0, leading to a pure detergent corona.

Even when working at 0.2% DDM, the SAXS signal of the free micelles is comparable with the signal from the protein−detergent complexes. A correct subtraction of the free detergent micelle signal is thus of crucial importance if one wants to analyze the protein conformation. In the present work, we took advantage of the online SEC−HPLC−SAXS−refractometry system available on the SWING beamline at SOLEIL. The correct subtraction of the free micelle signal was then possible by recording the SAXS signal just prior to the elution of the protein. Furthermore, the setup also (i) ensures that the resulting signals are not affected by the possible presence of aggregates and (ii) allows precise quantification of the detergent composition of the complex by independent experimental techniques.

How Many Detergent Molecules Surround One Aquaporin-0? Using three independent methods, we obtained a consistent estimate of N_{det}, the number of detergent molecules surrounding aquaporin-0. Using the value of the SAXS intensity extrapolated to $Q = 0$, N_{det} = 211 ± 10; the RI measurement, N_{det} = 238 ± 15; and from the coarse-grained model, N_{det} = 271 ± 30. The first two methods are very dependent on the accuracy of reference values. In the $I(0)/C$ method, the value of N_{det} is quite sensitive to the partial specific volumes of both the detergent and the protein. For DDM, the values of $\bar{v}_{det}$ found in the literature[14] range from 0.800 to 0.837 $cm^3 \cdot g^{-1}$, corresponding to a N_{det} value between 168 and 211. For the refractometry measurement, the RI increments (dn/dc) contribute a considerable uncertainty. Typical values for detergents vary between 0.10 and 0.16 $mL \cdot g^{-1}$, and while the value of 0.143 $mL \cdot g^{-1}$ is often accepted for DDM, values from 0.134 to 0.147 $mL \cdot g^{-1}$ have been reported,[12,27] and the RI increment of AQP0 has a comparable uncertainty. Finally, in both methods a small error in protein−detergent complex concentration can also alter N_{det}. In contrast, the coarse-grained model determination of N_{det} is independent of external parameters, as it depends only on the shape of scattering curve. One could object that the result may be strongly model-dependent. However, we can emphasize that (i) the error bars were calculated by reducing the constraints on the agreement between calculated and experimental SAXS curves to χ/χ_{min} = 1.7, and (ii) for the best circular torus model, N_{det} = 275, which is practically the same as for the elliptical model. Moreover, the DDM partial specific volume extracted from the coarse-grained model, 0.845 ± 0.005 $cm^3 \cdot g^{-1}$, is very close to the accepted value of 0.837 $cm^3 \cdot g^{-1}$.

The number of detergent molecules surrounding a membrane protein depends strongly on both the type of detergent and the protein (proteins with a large hydrophobic area should be surrounded by more detergent). Previous studies of different membrane proteins (bacteriorhodopsin, calcium ATP_{ase}, reaction center, and cytochrome oxidase)[27] have reported detergent binding capacities from 77 to 330 molecules. The value reported in the present work is consistent with these results.

Coarse-Grained Simulation. The coarse-grained structural model proposed in this work, is based on four independent parameters reflecting the geometry of the corona (*a*, *b*, *e*, and *t*) and two extra fitting parameters arising from the program Crysol: the parameter which slightly optimizes the electronic densities and the hydration layer density contrast. A similar geometrical model has already been proposed to mimic the organization of detergent around a membrane protein.[12] However, for that study the very low signal-to-noise ratio for $q > 0.1$ $Å^{-1}$ in the raw data prevented a precise determination of the detergent corona shape. In our work, the shape of the detergent corona model (Figure 4) is fully consistent with previous studies. First, the parameter representing the thickness of the hydrophilic region, t = 5.5 Å, is very similar to the reported value of 6−6.3 Å for pure DDM micelles.[19] Second, the thickness of the corona along the membrane normal (z direction), $a + 2t$ = 42 Å in our notation, lies well within the typical range of 30−55 Å previously reported for lipid bilayer thicknesses and also matches the approximately 30 Å hydrophobic belt of AQP0.[26] The detergent corona radius (or size of the corona in the y direction, b = 36 Å) is more

dx.doi.org/10.1021/ja301667n | J. Am. Chem. Soc. 2012, 134, 10080−10088

difficult to compare to previous studies as it necessarily depends on the size of the membrane protein at the center of the protein−detergent complex. In the case of pure detergent micelles of DDM, the disk radius was found to be equal to 29 Å.[19] However, as the organization of detergent around membrane proteins will differ from pure micelles, we can only note that the micelle radius is comparable with the radius of the protein suggesting that the detergent torus does not expand far from the protein.

The electron densities of the detergent headgroup and tail were optimized by the program Crysol through the adjustment of the parameter α. The optimal electron densities of 0.515 and 0.275 e/Å^3 differ by less than 3% from the values previously published for free DDM micelles[19] or DM surrounding a membrane protein.[12] In conclusion, the geometrical shape, the electron densities, and the partial specific volumes obtained from the model are compatible with the known physical and chemical characteristics of DDM.

Elliptical versus Circular Shape. Several theories and models for the detergent organization around membrane proteins have been proposed in the recent years, and models of circular[12] and elliptical[28,29] coronas of detergent have frequently been compared. In other cases, synthetic bilayers such as nanodiscs that were thought to be circular were found to have SAXS profiles that were better fitted by an elliptical shape.[29] In the present work, the experimental data shown in Figure 4 is better fitted by an elliptical detergent corona than a circular one, although the optimal ellipticity (e = 1.12) corresponds to a corona that is only slightly distorted from a circle (e = 1). However, we do not claim that the detergent corona is in a static elliptical conformation. Indeed, it is important to recall that SAXS data probe the average conformation of an object and the elliptical conformation of the model can instead be interpreted in terms of dynamical behavior of the detergent corona. If the detergent corona underwent large conformational fluctuations, at each point in time the corona would have an elliptical shape oriented at a random in the xy plane. SAXS would not distinguish between these different orientations and just retain the average shape. Similarly, polydispersity in the corona size cannot be excluded and even if the coronas are individually circular, the average model would probably result in an ellipsoidal shape. At least, we may argue that if such polydispersity exists, it is certainly dynamical and not static. Otherwise a variation in the SAXS curve would have appeared along the elution profile, which does not occur, as seen from Figure SI3b.

SAXS versus SANS. Most of the recent structural studies of membrane proteins in detergent solution have used small-angle neutron scattering (SANS) instead of SAXS. With neutron scattering, it is possible to match the scattering density of the detergent by simply modulating the D_2O/H_2O ratio in the buffer. The resulting curve from a detergent−protein therefore essentially reflects the structure of the protein alone, making possible the use of ab initio structural modeling.[30−33] The protein itself can be partially deuterated, thus providing the extra possibility to differentiate its signal from that of an associated partner, as nicely shown by Clifton et al.[32]

However, despite such studies provide protein low resolution envelopes fully compatible with the data, it is striking to note that no successful direct comparison between a known crystal structure and a SANS curve has been published. The most probable reason is that even if detergent scattering can be exactly matched at Q = 0, scattering contributions, though small, still remain at finite Q values. Hence, the SANS curve does not exactly represent the pure protein contribution. While SANS is certainly essential to determine a first hint of a membrane protein shape, modeling from SAXS data can more profoundly benefit from high resolution information. In turn, subtle changes in the scattering curves, due to external conditions, can be expected to be more easily interpretable in terms of conformational changes.

Implication for Proteins of Unknown Structure. The protocol developed here applies to membrane proteins of known structure. It is clearly expected to be particularly useful to monitor conformational changes rather than determine unknown low resolution structures. Yet, by improving our knowledge about the corona structures of different proteins, we may reasonably expect to derive rules that could in turn be applied to membrane protein structures derived from folding predictors like Rosetta[34] or I-Tasser.[35] In this way, SAXS can become a precise and indispensable technique to accompany these applications for a better selection in their *ab initio* high-resolution structure determination.

CONCLUSION

Until recently, the arrangement and association of the detergent molecules surrounding a membrane protein was poorly understood. However, the growing interest in membrane protein structure and the difficulty studying conformational changes for this class of proteins has driven the development of new structural techniques. Approaches that study solubilized membranes proteins require an understanding of the detergent organization around the membrane proteins. Our work demonstrates the feasibility and usefulness of SAXS to characterize membrane proteins solubilized in detergent. The detergent corona around AQP0 can be effectively described using a coarse-grained modeling, and the combination with HPLC and refractometry allows deriving a consistent estimation of the number of detergent molecules in the complex. The resolution of this technical issue opens a route to more detailed structural studies of membrane proteins.

ASSOCIATED CONTENT

Supporting Information

Structure and chemical formula of the DMM molecule; validation of the coarse-grained approach by comparison with an analytical model; display of individual SAXS frames; χ values and scattering curves from non-optimized models. This material is available free of charge via the Internet at http://pubs.acs.org.

AUTHOR INFORMATION

Corresponding Author

javier.perez@synchrotron-soleil.fr

Author Contributions

‡J.P. and S.M. contributed equally.

Notes

The authors declare no competing financial interest.

ACKNOWLEDGMENTS

This work was supported by the CNRS "Interface physique, biologie et chimie: soutien à la prise de risque". A.B. was supported by the Ecole Doctorale Interdisciplinaire pour le vivant (ED387, IviV). We thank Dominique Durand and Guillaume Evrard for extremely fruitful discussions. We thank

Gilman Tombes for the careful reading of the manuscript and comments. Finally, we are very grateful to Didier Mauchand (INRA, Jouy en Josas) for providing the lenses.

REFERENCES

(1) Wallin, E.; Heijne, G. V. *Protein Sci.* **1998**, *7*, 1029.
(2) Terstappen, G. C.; Reggiani, A. *Trends Pharmacol. Sci.* **2001**, *22*, 23−26.
(3) Davey, J. *Exp. Opin. Ther. Targets* **2004**, *8*, 165−170.
(4) White, S. H. *Nature* **2009**, *459*, 344−346.
(5) Hilge, M.; Siegal, G.; Vuister, G. W.; Guntert, P.; Gloor, S. M.; Abrahams, J. P. *Nat. Struct. Mol. Biol.* **2003**, *10*, 468.
(6) Shimaoka, M.; Takagi, J.; Springer, T. A. *Annu. Rev. Biophys. Biophys. Chem.* **2002**, *31*, 485.
(7) Srivastava, J.; Barber, D. L.; Jacobson, M. P. *Physiology* **2007**, *22*, 30.
(8) Svergun, D.; Koch, M. *Rep. Prog. Phys.* **2003**, *66*, 1735−1782.
(9) Putnam, C. D.; Hammel, M.; Hura, G. L.; Tainer, J. *Q. Rev. Biophys.* **2007**, *40*, 191−285.
(10) Hura, G. L.; Menon, A. L.; Hammel, M.; Rambo, R. P.; Poole, F. L.; Tsutakawa, S. E.; Jenney, F. E.; Classen, S., Jr.; Frankel, K. A.; Hopkins, R. C. *Nat. Methods* **2009**, *6*, 606−612.
(11) Grossmann, J. G. *J. Appl. Crystallogr.* **2007**, *40*, s217−s222.
(12) Mo, Y.; Lee, B.-K.; Ankner, J. F.; Becker, J. M.; Heller, W. T *J. Phys. Chem. B* **2008**, *112*, 13349−13354.
(13) O'Neill, H.; Heller, W. T.; Helton, K. E.; Urban, V. S.; Greenbaum, E. *J. Phys. Chem. B* **2007**, *111*, 4211−4219.
(14) le Maire, M.; Arnou, B.; Olesen, C.; Georgin, D.; Ebel, C.; Møller, J. V. *Nat. Protoc.* **2008**, *3*, 1782−1795.
(15) Hasler, L.; Walz, T.; Tittmann, P.; Gross, H.; Kistler, J.; Engel, A. *J. Mol. Biol.* **1998**, *279*, 855−864.
(16) VanAken, T.; Foxall-VanAken, S.; Castleman, S.; Ferguson-Miller, S. *Methods Enzymol.* **1986**, *125*, 27−35.
(17) Gonen, T.; Cheng, Y.; Kistler, J.; Walz, T. *J. Mol. Biol.* **2004**, *342*, 1337−1345.
(18) David, G.; Pérez, J. *J. Appl. Crystallogr.* **2009**, *42*, 892−900.
(19) Lipfert, J.; Columbus, L.; Chu, V. B.; Lesley, S. A.; Doniach, S. *J. Phys. Chem. B* **2007**, *111*, 12427−12438.
(20) Guinier, A. *Ann. Phys.* **1939**, *12*, 161−237.
(21) Wilson., C. B. *J. Polym. Sci.* **1993**, *19*, 594−594.
(22) Svergun, D.; Barberato, C.; Koch, M. H. *J. Appl. Crystallogr.* **1995**, *28*, 768−773.
(23) Ebel, C. *Methods* **2011**, *54*, 56−66.
(24) Salvay, A. G.; Ebel, C. *Prog. Colloid Polym. Sci.* **2006**, *131*, 74−82.
(25) Prive, G. G. *Methods* **2007**, *41*, 388−397.
(26) Hite, R. K.; Li, Z.; Walz, T. *EMBO J.* **2010**, *29*, 1652−1658.
(27) Møller, J. V.; le Maire, M. *J. Biol. Chem.* **1993**, *268*, 18659−18672.
(28) le Maire, M.; Champeil, P.; Møller, J. *Biochim. Biophys. Acta* **2000**, *1508*, 86−111.
(29) Skar-Gislinge, N.; Simonsen, J. B.; Mortensen, K.; Feidenhans'l, R.; Sligar, S. G.; Lindberg Møller, B.; Bjørnholm, T.; Arleth, L. *J. Am. Chem. Soc.* **2010**, *132*, 13713−13722.
(30) Nogales, A.; García, C.; Pérez, J.; Callow, P.; Ezquerra, T. A.; González-Rodríguez, J. *J. Phys. Chem.* **2010**, *285*, 1023−1031.
(31) Johs, A.; Hammel, M.; Waldner, I.; May, R. P.; Laggner, P.; Prassl, R. *J. Phys. Chem.* **2006**, *281*, 19732−19739.
(32) Clifton, L. A.; Johnson, C. L.; Solovyova, A. S.; Callow, P.; Weiss, K. L.; Ridley, H.; Le Brun, A. P.; Kinane, C. J.; Webster, J. R. P.; Holt, S. A.; Lakey, J. H. *J. Phys. Chem.* **2012**, *287*, 337−346.
(33) Cardoso, M. B.; Smolensky, D.; Heller, W. T.; O'Neill, H. *J. Phys. Chem. B* **2009**, *113*, 16377−16383.
(34) Das, R.; Baker, D. *Annu. Rev. Biochem.* **2008**, *77*, 363−382.
(35) Roy, A.; Kucukural, A.; Zhang, Y. *Nat. Protoc.* **2010**, *5*, 725−738.